

# ALIGNED-GRID VALVES

## Distribution of Current Density

By D. C. Rogers, A.M.I.E.E.

(Standard Telephones and Cables, Ltd.)

**SUMMARY.**—The electron beam from the cathode of an amplifier valve is focused into well-defined beams by the action of the electric field in the region of the control grid. In aligned-grid valves, use is made of this phenomenon by placing the screen-grid wires in positions where they will intercept only a small fraction of the total cathode current.

Owing to the doubtful validity of the existing theoretical treatment of the subject, an experimental study of the current-density distribution in these electron beams was undertaken for the purpose of determining the best position of the screen wires.

It is often assumed that the grid-to-screen distance should be such that the focus of the electron beam lies in the plane of the screen. The measurements described here show that this is not necessarily true and that a lower screen current will usually be obtained with a smaller grid-to-screen distance.

### LIST OF SYMBOLS

- $a$  = Grid pitch, measured between centres of grid wires.  
 $d$  = Grid-wire diameter,  
 $l_g$  = Cathode-grid distance.  
 $l_a$  = Cathode-anode distance in a triode, or cathode-screen distance in a tetrode.  
 $l_a - l_g$  = Grid-anode distance in a triode, or grid-screen distance in a tetrode.  
 $V_g$  = Grid potential with respect to cathode (e.s.u.)  
 $V_a$  = Anode potential of a triode or screen voltage of a tetrode with respect to cathode. (e.s.u.)  
 $V_o$  = Potential in the grid plane. (e.s.u.)  
 $e$  = Electron charge (e.s.u.)  
 $m$  = Electron mass.  
 $I$  = Current flowing between two grid wires, per unit length of grid wire. (e.s.u.)  
 $J$  = Cathode-current density (e.s.u.)  
 $y$  = Distance co-ordinate measured parallel to the cathode surface and perpendicular to the grid wires.  
 $z$  = Distance co-ordinate measured perpendicular to the cathode surface.  
 $V_a$  = The anode potential of an equivalent diode (e.s.u.) (See Appendix I.)  
 $s$  = The cathode-anode distance of an equivalent diode. (See Appendix I.)  
 $v$  = Electron velocity (cm/sec)  
 $t$  = Time in seconds.  
 $\mathcal{E}$  = Electrostatic field (e.s.u.)  
 $\mu$  = Amplification factor.

## 1. Introduction

IN pentode or beam tetrode valves, it is often found that the power-handling capacity is limited by the maximum permissible screen-grid dissipation and, accordingly, much attention has been devoted to the positioning of the screen wires in the shadow of those of the control grid, in order to intercept a minimum fraction of the cathode current. In receiving-type amplifying valves, too, the reduc-

tion of screen current is of considerable importance since the noise current generated by such valves is largely dependent on the amount of current falling on the screen.

It has long been known that in the useful operating range of most valves the electrostatic field in the region of the control-grid causes the electrons to be deflected towards a plane midway between the grid wires. Some typical electron paths in the cathode-grid and grid-screen regions are shown in Fig. 1. Bull<sup>1</sup> has shown that the apertures between the grid wires form cylindrical electron lenses and has shown how their focal lengths can be determined, using the method of Davissou and Calbick<sup>2,3</sup>.

In practice it is found that the screen current is not reduced to zero, as would be expected if the electron beams came to perfect foci; this fact could be attributed

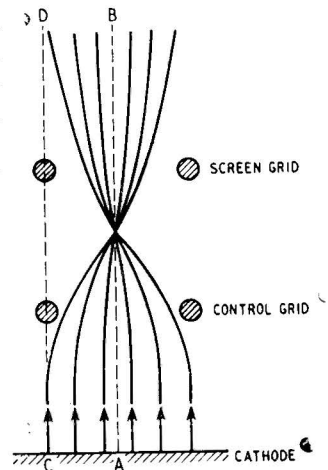


Fig. 1. Typical electron paths in an aligned-grid valve.

to one or more of the following causes:

- The lenses formed by the grid apertures possess large aberrations.
- The mutual repulsion between electrons, due to their charge, causes a tendency for the beam to diverge in the grid-screen region.
- The electrons are emitted from the cathode with finite velocities, distributed according to the Maxwell law.

MS accepted by the Editor, June 1949

(d) The electrostatic field configuration in the vicinity of the screen grid is such as to deflect the electrons towards the screen wires.

In Appendix I it is shown that the space-charge effect mentioned in (b) above is insufficient to account for observed screen currents, and it can readily be demonstrated (for example, by observing the variation in the proportion of cathode current intercepted by the screen as the cathode temperature is varied) that electron emission velocity is also not a major cause of the spread of the beams. It must therefore be concluded that the screen currents obtained in practice result from the existence of large aberrations in the lenses, from the effect of the electrostatic field in the screen region, or from both these causes.

Now the method employed by Bull to determine the focal length is, as he points out, valid only for electrons travelling close to the central plane AB (Fig. 1). It is clear, however, that the screen current does not arise from these electrons, but from those passing very near to the control-grid wires and we are, therefore, justified in asking whether the focal plane is, in fact, the optimum position for the screen. In view of the difficulty of obtaining an analytical solution for the trajectories of electrons passing near the control-grid wires, involving as it would

with a narrow slot, the current passing through the slot thus being a measure of the current density falling on the plate. The measured distribution is, therefore, that appertaining to a particular cathode-grid geometry and grid-screen distance, and does not include the localized effect around the screen wires. The measurements were carried out for a range of grid-screen distances and with various cathode-grid geometries.

It should be noticed that while this method enables the optimum screen position to be determined, it does not enable the screen current at this position to be predicted. The screen current will, in general, depend on the conditions obtaining in the screen-anode region (e.g., the potential and location of the anode and the space-charge conditions in the intervening space)

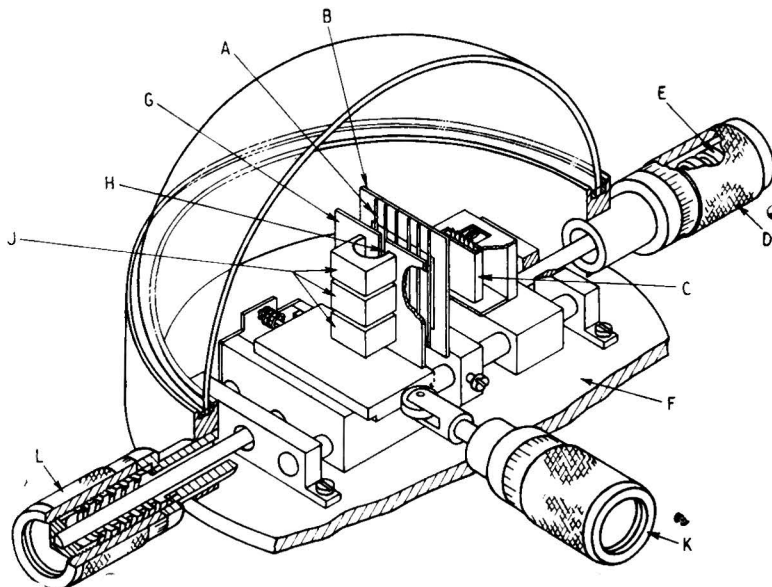


Fig. 2. Simplified sketch of experimental valve.

consideration of the effect of space charge on the field in the grid region, it was decided that an experimental approach would be profitable. The investigation to be described here was accordingly undertaken; viz., an investigation of the distribution of current density in the plane of the screen.

This current density distribution depends on the trajectories of individual electrons in their flight from the cathode to the screen plane, and hence on the field configuration in the grid region. It does not depend appreciably on the geometry of the screen, except in the immediate proximity of a screen wire, since the field irregularities do not extend far into the grid-screen space. In making these measurements, details of which are given in a later section, the screen was replaced by a solid metal plate provided

as well as on the diameter and spacing of the screen wires.

## 2. Experimental Procedure

The measurements were made on a continuously-evacuated demountable valve in which the electrodes could be moved by manipulation of external micrometer controls while the valve was in operation. In the interests of simplicity attention has been confined to parallel plane electrode structures. However, little error should arise in the application of the results to practical valve designs, since the grid-support rods effectively divide the valve into two sections, each of which approximates roughly to a parallel plane structure.

A simplified sketch of the apparatus is shown in Fig. 2. The grid consisted of straight molyb-

denum wires A welded to a rectangular steel frame B. The cathode C was of the indirectly-heated oxide-coated nickel type, the coated area being a flat face 13 mm × 10 mm. The cathode-grid distance could be adjusted by means of the micrometer screw D. The vacuum was maintained by the flexible metal bellows E soldered to the metal envelope F of the valve.

As mentioned in the introduction, the screen was replaced by a flat metal plate, shown at G in the figure. This plate was provided with a slot H, 0.1-mm wide, parallel to the grid wires, behind which was located a collector electrode J, operated at a positive potential of 150 volts with respect to the anode G. The current flowing to this collector electrode was a measure of the current density falling on the anode plate. The whole plate could be moved in a direction parallel to the grid plane and perpendicular to the grid wires by the micrometer screw K. Thus by observing the variation of the collector current as the slot in the anode was moved from a position behind one grid wire to behind the next, the variation in current density across the electron beam could be determined.

The anode-grid spacing was also variable and was controlled by micrometer L. In order to avoid spurious effects at the ends of the slot, the collector was divided into three sections as shown, and measurements were made of the current to the centre section only, the outer two sections being maintained at the same potential as the centre section. Since under some conditions the current reaching the collector amounted to a few microamperes only out of a total cathode current of 4 mA it was necessary to prevent electrons from reaching the collector by other than the intended paths; for instance, by secondary emission from various parts of the apparatus. This was accomplished by suitably placed shields at cathode potential; these have been omitted from Fig. 2 for the sake of clarity.

The experimental procedure was to scan the beam emerging from the centre grid aperture by moving the collector slot transversely and measuring the collector current at intervals of 0.1 mm. This process was repeated for various anode-grid distances, the total anode current being maintained constant at 4 mA by adjusting the anode voltage. Because of the large number of variables that would otherwise be involved, measurements have been made with the grid at cathode potential only. A curve showing the ratio of the collector current at each point in the beam section to the average across the beam was plotted for each anode-grid distance. This ratio is equal to the ratio of the current density at that point to the average current density. A typical series of such curves is shown in Fig. 3.

It is readily shown that, provided the effects of initial emission velocity are negligible, the shapes of the electron trajectories are dependent only on the shape of the electrodes and not on the actual dimensions. Hence, any geometrical scaling factor can be used without changing the

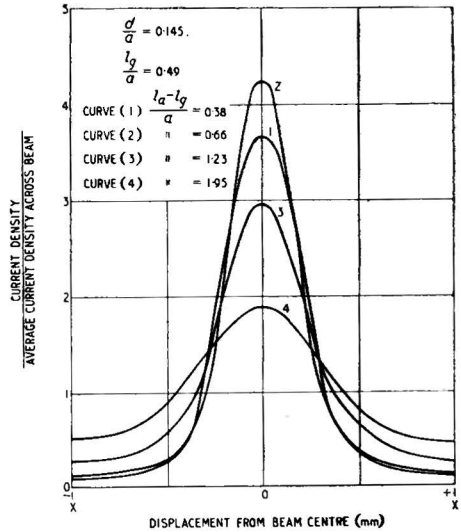


Fig. 3. Variation in current density across the electron beam.

relative distribution of current density. It is, therefore, convenient to maintain one dimension constant and to relate the other dimensions to this fixed dimension. In this case the grid pitch  $a$  was kept constant at 2 mm and other dimensions were in terms of grid pitch. The experiments were repeated for various values of the ratio  $l_g/a$  (cathode-grid distance/grid pitch) and  $d/a$  (grid-wire diameter/grid pitch) likely to be encountered in practice. (See also list of symbols).

The shape of the electron paths is dependent also on the ratio only of the electrode potentials and not on their magnitude. However, since the grid was maintained at cathode potential, this amounts to saying that the relative distribution of current density is independent of anode voltage.

### 3. Results and Their Significance

Referring again to Fig. 3, which shows a typical series of curves of current distribution in the anode plane (or in what would be the screen plane, were the valve a tetrode) it will be seen that, as would be expected, the current density rises from a minimum behind the grid wires to a maximum value midway between them.

These curves were obtained with  $d/a = 0.145$  and  $l_g/a = 0.49$ . As the ratio grid-anode distance/grid pitch,  $(l_a - l_g)/a$  is increased, the magnitude

of the maximum between the grid wires rises until it is itself a maximum and then falls again, the maximum in this case occurring when  $(l_a - l_g)/a = 0.65$ . This is made clearer by reference to Fig. 4, in which the dotted curve shows the variation with  $(l_a - l_g)/a$  in current density in the mid-plane between the grid wires; i.e., along the line AB, Fig. 1.

Quite obviously the value of  $(l_a - l_g)/a = 0.65$ , which gives a maximum in this curve, corresponds to the case when the focus of the electron beam is in the plane of the anode or, of course, the screen, had the valve been a tetrode. It is interesting to note that, with the electrode geometry corresponding to this point, the position of the focus as determined by Bull's method would have been at a distance  $0.45a$  from the grid plane.

Now let us examine the variation in current density behind the grid wires, and in the plane of the anode of the experimental triode (i.e., along the line CD, Fig. 1) as the anode-grid distance is varied. This current is given by the points X on the curves of Fig. 3, but is shown more clearly by the solid curve of Fig. 4, which has been plotted from Fig. 3. It will be seen that there is no minimum corresponding to the maximum occurring along AB, but rather that the current density increases progressively as the distance between grid and anode is increased.

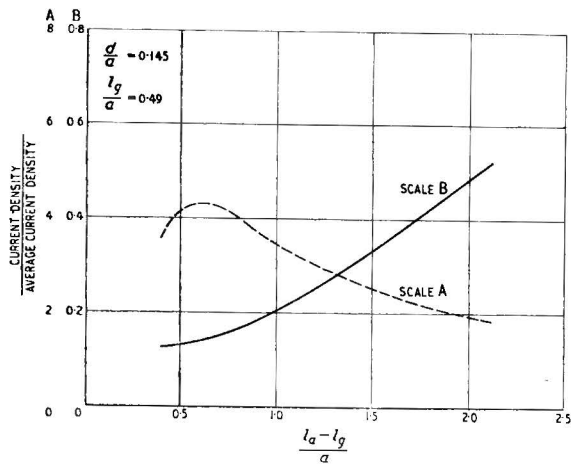


Fig. 4. Variation of current density along the line AB of Fig. 1 (dotted curve) and along the line CD (solid curve).

The implication of this is clearly that for minimum screen current, at least at zero grid voltage, the screen should be located as nearly as possible to the control grid, and not in the plane of the focus, as is frequently assumed. However, before considering this point further, the effect of varying the other valve dimensions will be described.

Fig. 5 shows a family of curves similar to those of Fig. 4, plotted for various values of the grid-wire diameter/grid pitch  $d/a$ . It will be seen that the value of  $(l_a - l_g)/a$  for which the beam focuses in the anode plane decreases as the grid-wire diameter is increased. This

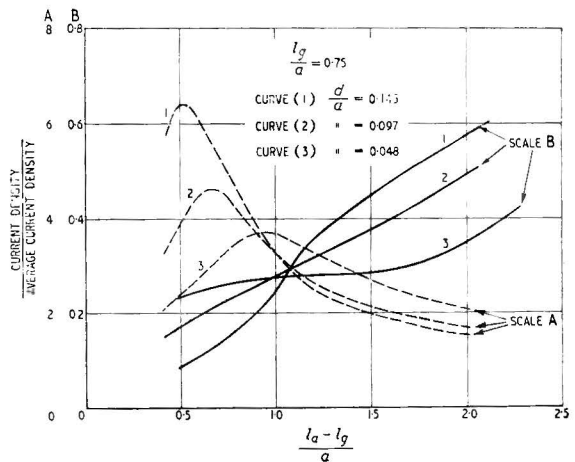


Fig. 5. Variation of current density along the line AB (dotted curves) and along the line CD (solid curves) for various values of  $d/a$ .

is also shown in Fig. 6, which shows the value of  $(l_a - l_g)/a$  for which the beam focuses in the anode plane versus the grid-wire diameter parameter  $d/a$ .

The effect on the current density behind the grid wires is, as shown in Fig. 5, that for small values of  $(l_a - l_g)/a$  the current density decreases with increasing wire diameter, while for large values of  $(l_a - l_g)/a$  the reverse is the case.

Fig. 7 shows another series of curves, also similar to Fig. 4, plotted for a constant grid-wire diameter, corresponding to  $d/a = 0.048$  and for varying cathode-grid distances. It will be seen that the value of  $(l_a - l_g)/a$  for focus in the anode plane is substantially independent of cathode-grid distance, but that the value of the current density maximum increases as the cathode-grid distance increases. It should be mentioned here that these maxima of current density may be quite appreciably in error, since the measuring slot has finite width, and this width may be greater than the width of the high-current-density part of the beam in cases where the focus is very sharp.

In Appendix II an expression is developed for the focal length of the lens formed by the grid apertures, using a similar method to that used by Bull, but based on electrostatic considerations only. The simplicity of the expression obtained in this way draws attention to the fact that the dominant feature in determining the focal length at zero grid voltage is the ratio of

grid-wire diameter to grid pitch, a fact which is strikingly confirmed by the measurements.

The expression obtained is

$$f = \frac{3}{2} f_o \left[ 1 + \frac{1}{6} \frac{f_o}{l_g} \right]$$

$$\text{where } f_o = \frac{a}{\pi} \log \frac{a}{\pi d} \quad \dots \quad (1)$$

In Fig. 6 the calculated value of  $f$  is plotted as a function of  $d/a$  for  $l_g/a = 0.75$ , the experimental results being shown for comparison. For reasons outlined in the appendix, the apparently good agreement between the calculated and measured values is probably due to a fortuitous cancellation of errors.

The effect of change in cathode-grid distance on the current density behind the grid wires is also shown in Fig. 7. At small values of  $(l_a - l_g)/a$  the current density decreases with increase of  $l_g/a$ , while with larger values of  $(l_a - l_g)/a$ , it increases with  $l_g/a$ .

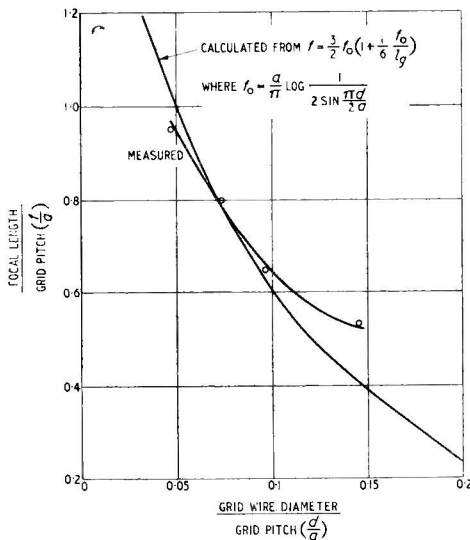


Fig. 6. Value of  $(l_a - l_g)/a$  for which the beam focuses in the anode plane: both curves relate to  $l_g/a = 0.75$ .

An interesting series of curves is shown in Fig. 8. These are similar to Fig. 3, and show the current-density distribution across the electron-beam section for thin grid wires. When the anode is very close to the grid [i.e., for  $(l_a - l_g)/a$  small] the distribution of current is seen to take the shape of a double-humped curve. This provides additional confirmation, if any is necessary, that the lenses formed by the grid apertures have large aberrations, for it is clear that in this case the outer electrons of the beam are subject to a stronger lens action than those in the centre,

resulting in a 'crowding' of electrons at the outer edges of the beam.

Let us now consider whether these results can be applied to the design of a practical valve with reduced screen current. The results apply only to zero grid voltage, of course, whereas in

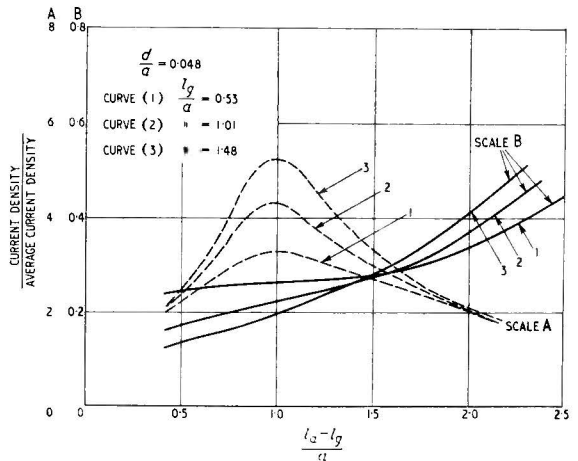


Fig. 7. Variation of current density along the line AB of Fig. 1 (dotted curve) and along the line CD (solid curves) for various values of  $l_g/a$ .

use the valve will normally have an alternating voltage applied to the grid, and it is the average screen current over the grid-voltage cycle which must be minimized. However, if we confine our attention to amplifiers in which the grid is not driven positive, the conditions for minimum average screen dissipation and minimum dissipation at the instantaneous current maximum would not be expected to be very different.

It is clear from Figs. 3 and 4 that to intercept the minimum cathode current, the screen-grid wires should be as near to the control grid as possible. Reducing the control-grid-to-screen distance will also have the effect of reducing the grid-to-screen amplification factor of the valve, and since, in general, it will be necessary for the static characteristics of the valve to be within specified limits it will be necessary to correct this reduction in amplification factor by increasing the diameter of the grid wires. As shown in Fig. 5, if the grid-screen distance is less than the grid pitch, the effect of large diameter grid wires will be to reduce the screen current still further. Fig. 7 shows that, with large grid wires and small grid-screen distances, the screen current will not vary rapidly with cathode-grid distance, and hence this distance need depend only on the static characteristic requirements.

The limit to the reduction in control-grid-to-screen distance is set by practical considerations. Also, when the cathode-grid distance is small, a

small grid-to-screen distance and large diameter grid wire result in non-uniformity of the field at the cathode and consequent increased curvature of the grid-volts-anode-current characteristics.

It will be appreciated that even if these findings were applicable to positive grid voltages, they would not be of much value. A grid of large diameter wires operated at a positive voltage would itself intercept an intolerably high proportion of the cathode current.

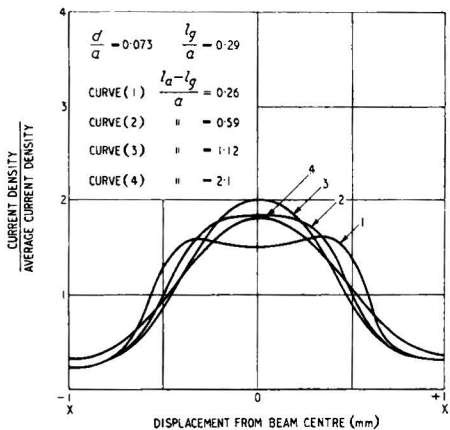


Fig. 8. Variation of current density across beam section for thin grid wires and small value of  $l_g/a$ .

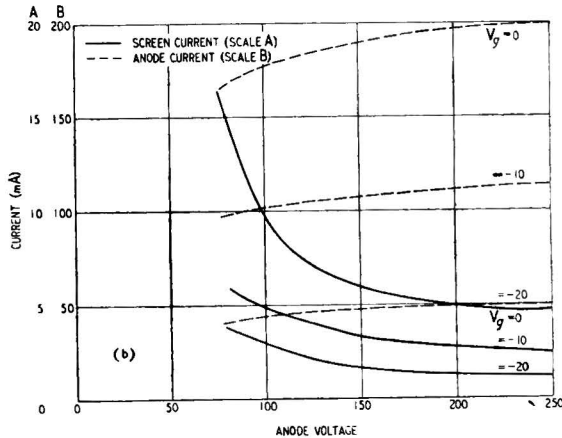
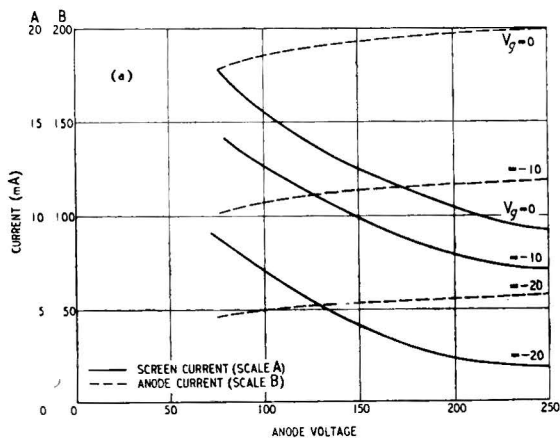


Fig. 9. Screen and anode currents of (a) valve similar to the Type 807 at 250-V screen-grid potential; (b) valve with thicker grid wires and decreased grid-to-screen distance; screen-grid potential = 200 V.

Next let us consider whether the results of these experiments can be used to predict the screen current when the valve geometry is known. It is convenient to regard the screen current as consisting of two components, a forward component arriving from the cathode-grid region, and a reverse component consisting of electrons returned from the screen-anode region. The first-mentioned component will be determined by

the current density flowing in the region in which the screen wire is located, and by the shape of the electrostatic field in the immediate vicinity of the screen wire. Spangenberg<sup>4</sup>, in a theoretical investigation of the positive-grid triode, has shown that in the case of equal grid and anode voltages the positive grid may be considered to intercept current over an area that normally lies between 1.25 and 1.8 of the projected area of the wire. It is possible that Spangenberg's method could be adapted to give an approximate solution for the tetrode, by considering the tetrode control-grid plane as the cathode of Spangenberg's triode, but since the method is based on electrostatic considerations only, it could not be used when the space-charge in the screen-anode region is appreciable. It could be applied, therefore, only to the case of small screen-to-anode distance and high anode voltage, and would not be valid in the more interesting case of the tetrode in which space-charge in the screen-anode region is used to suppress secondary emission from the anode. Furthermore, the process of treating the control grid as the electron source would be valid only for large grid-to-screen distances, whereas it has been proposed above that the method of reducing screen current is to reduce this distance.

The other component of screen current (viz., that returned from the screen-anode region)

will depend only on conditions existing beyond the screen. In most beam tetrodes this component will predominate only at very low anode voltages, while the first-mentioned component will predominate at high anode voltages. Any improvement effected by reducing the control-grid-to-screen distance will, therefore, be apparent mainly at high anode voltages.

In order to verify the general conclusions

reached, the following experiment was carried out. A valve was made similar to the type 807 beam power tetrode, but in which the ratio screen-grid distance/grid pitch was reduced from 1.49 to 0.58 and the grid-wire diameter was increased such that  $d/a$  was 0.192 instead of 0.096 for the normal valve. It was hoped in this way to make a valve having similar characteristics to the 807 in the negative-grid region, but with reduced screen current. In the modified valve, the screen current was 5.0 mA at  $V_a = 250$  V,  $V_{g1} = 0$ ,  $I_a = 200$  mA. ( $I_a$  set to 200 mA by adjusting the screen voltage), compared with 10 mA for the normal valve. Owing to the fact that the increase in grid-wire diameter did not quite compensate for the decrease in grid-screen distance, the anode current of 200 mA was obtained at a somewhat lower screen voltage than normal; viz., 200 V instead of 250 V. This resulted in the space-charge conditions in the screen-anode space being altered with a consequent slight change in the shape of the anode-volts-anode-current curve. The characteristic curves of the modified and the normal valve are shown in Figs. 9(a) and (b) respectively for comparison. In the modified valve, some increase in the curvature of the grid-voltage-anode-current characteristic was noticeable.

#### 4. Conclusion

These experiments have shown that some reduction in the screen current in an aligned-grid valve should be possible by the use of a smaller grid-to-screen distance than is common at present, provided this reduced spacing is not incompatible with conditions set by other characteristics of the valve. This conclusion is in accord with physical reasoning, for it is clear that there must be regions of very low current density immediately behind the control-grid wires, since the only electrons able to reach these regions—apart, of course, from those returned from the screen-anode space at low anode voltages—are those suffering deflections of nearly  $90^\circ$  at the control grid.

#### 5. Acknowledgment

The author wishes to thank Mr. M. T. G. Chick for valuable assistance in the experimental work, and Messrs. Standard Telephones & Cables Limited for permission to publish this paper.

#### APPENDIX I

##### Space-charge defocusing.

This appendix is intended to show that defocusing of the electron beams, due to space charge, does not cause appreciable spreading of the beam. It is con-

venient to consider the case of an aberration-free lens of such focal length that the beam would form a line focus in the plane of the screen in the absence of space-charge. The presence of space-charge will cause the beam to have finite thickness in the screen plane, and it is our aim to find this beam thickness.

An electron will emerge from the grid plane with a velocity  $v_z$  given by

$$v_z = \sqrt{\frac{2eV_o}{m}} \quad \dots \quad (2)$$

where  $V_o$  is the effective potential in the grid plane in electrostatic units.

The electron then travels under the influence of an accelerating field towards the anode. This field will be assumed uniform and equal to

$$\mathcal{E} = \frac{V_a - V_o}{l_a - l_g} \text{ electrostatic units} \quad \dots \quad (3)$$

The distance travelled in time  $t$  is

$$\sqrt{\frac{2eV_o}{m}} t + \frac{1}{2} \frac{e}{m} \frac{(V_a - V_o) t^2}{(l_a - l_g)} \text{ cm} \quad \dots \quad (4)$$

so that the time  $t_o$  taken to reach the screen plane is given by

$$(l_a - l_g) = \sqrt{\frac{2eV_o}{m}} t + \frac{1}{2} \frac{e}{m} \frac{(V_a - V_o) t^2}{(l_a - l_g)} \quad \dots \quad (5)$$

whence

$$t_o = \sqrt{\frac{2m}{e} \frac{(\sqrt{V_a} - \sqrt{V_o})(l_a - l_g)}{(V_a - V_o)}} \quad \dots \quad (6)$$

Now the 'half-width'  $y_t$  of the beam at time  $t$  is given by Thompson and Headrich.<sup>5</sup> Expressed in the symbols used here it is:

$$y_t = y_o - v_y t + 2\pi I v_z \frac{m}{e} \frac{(l_a - l_g)^2}{(V_a - V_o)^2} \left( 1 + \frac{(V_a - V_o)et}{v_z(l_a - l_g)m} \right) \left[ \log \left( 1 + \frac{(V_a - V_o)et}{v_z(l_a - l_g)m} \right) - 1 \right] + \frac{2\pi I v_z (l_a - l_g)^2 m}{(V_a - V_o)^2 e} \quad (7)$$

where  $y_o$  is the initial 'half-width' of the beam,

$I$  is the current in the beam per cm of beam breadth; i.e., measured parallel to the cathode and to the grid wires,

$v_y$  is the initial velocity of the outermost electrons in a direction perpendicular to the grid wires and to the cathode face.

If the focal length of the lens is such that, in the absence of space-charge, a line focus would be formed in the screen plane,

$$y_o = v_y t_o \quad \dots \quad (8)$$

Now substituting in (7) for  $v_z$ ,  $t_o$ , and  $v_y$  from (2), (6) and (8) and rearranging, we get

$$y_{t_o} = -\frac{2\pi I \sqrt{\frac{2mV_o}{e}} (l_a - l_g)^2}{(V_a - V_o)^2} \left\{ \sqrt{\frac{V_a}{V_o}} \left[ \log \frac{V_a}{V_o} - 1 \right] + 1 \right\} \quad (9)$$

Hence the ratio total beam width/grid pitch

$$= 2y_{10}/a$$

$$= \frac{4\pi J \sqrt{\frac{2e}{m}} \sqrt{V_o} (l_a - l_g)^2 \left\{ \frac{\sqrt{V_a}}{\sqrt{V_o}} \left[ \log \frac{\sqrt{V_a}}{\sqrt{V_o}} - 1 \right] + 1 \right\}}{(V_a - V_o)^2} \quad (10)$$

where  $J$  is the average current density over the cathode surface ;

$$\text{i.e., } J = \frac{I}{a} \quad \dots \quad (11)$$

It is well known that

$$J = \frac{\sqrt{2}}{9\pi} \sqrt{\frac{e}{m}} \frac{V_D^{3/2}}{S^2} \quad \dots \quad (12)$$

where  $V_D$  is the effective anode potential of the so-called equivalent diode and  $S$  is the effective cathode-anode distance of this diode.

The values of  $V_D$  and  $S$  have been the subject of much discussion. It will be sufficiently accurate here to take

$$V_D = V_g + V_a/\mu \quad \dots \quad (13)$$

and

$$S = l_g + l_a/\mu \quad \dots \quad (14)$$

Substituting for  $J$  from (12), (13) and (14) and considering the case when  $V_g = 0$ , we obtain

$$2y/a = \frac{8}{9\mu^3} \frac{(l_a - l_g)^2}{(1 - V_o/V_a)^2 (l_g + l_a/\mu)^2} \left[ \left( \log \sqrt{\frac{V_a}{V_o}} \right) + \sqrt{\frac{V_o}{V_a}} - 1 \right] \quad \dots \quad (15)$$

$\frac{V_o}{V_a}$  can be obtained by Bull's method<sup>1</sup> or, alternatively,

from electrostatic considerations only, from Appendix II, equation (17).

For example, when  $l_a = 3l_g$

$$a = l_g$$

$$d/a = 0.1$$

$$\text{then } \mu = 10.6$$

$$\text{and } V_o/V_a = 0.0735$$

so that  $2y/a = 0.042$ .

It is thus clear that the beam spread, due to space-charge, is not sufficient to account for the values of screen current observed in practice.

## APPENDIX II

Davisson & Calbick's equation for the focal length of a cylindrical electrostatic lens is

$$\frac{1}{f_o} = \frac{\mathcal{E}_2 - \mathcal{E}_1}{2V_o} \quad \dots \quad (16)$$

where  $V_o$  is the potential in the aperture, and  $\mathcal{E}_1$  and  $\mathcal{E}_2$  are the fields on the entrance and exit sides of the lens respectively.

The effective potential in the grid-plane of a parallel plane triode at zero grid voltage is given by

$$V_o = V_a \frac{l_g}{l_a + \mu l_g} \quad \dots \quad (17)$$

provided the interelectrode spacings are not small compared with the grid pitch. The relevant values of  $\mathcal{E}_1$  and  $\mathcal{E}_2$  are those at the cathode and anode, respectively.

$$\text{Hence } \mathcal{E}_1 = \frac{V_o}{l_g} = \frac{V_a}{l_a + \mu l_g} \quad \dots \quad (18)$$

$$\text{and } \mathcal{E}_2 = \frac{V_a - V_o}{l_a - l_g} = \frac{V_a}{l_a - l_g} \left( 1 - \frac{l_g}{l_a + \mu l_g} \right) \quad (19)$$

From (16), (17), (18) and (19), we obtain after simplification

$$f_o = \frac{2(l_a - l_g)}{\mu} \quad \dots \quad (20)$$

For moderately thin grid wires,

$$\mu = \frac{2\pi(l_a - l_g)}{a \log \frac{1}{2 \sin \frac{\pi d}{2a}}} \quad \dots \quad (21)$$

$$\text{whence } f_o = \frac{a}{\pi} \log \frac{1}{2 \sin \frac{\pi d}{2a}} \quad \dots \quad (22)$$

In this expression  $f_o$  is the focal length of the lens formed by a grid aperture. This focal length is not the distance between the grid plane and the line focus of the beam, however, since, after leaving the lens region, the electrons travel along parabolic paths under the influence of a uniform accelerating field.

The distance  $f$  from the lens to the point where the beam focuses is shown by Bull to be

$$f = f_o \left[ 1 + \frac{1}{4} \frac{f_o}{(l_a - l_g)} \left( \frac{V_a}{V_o} - 1 \right) \right] \quad \dots \quad (23)$$

$$= f_o \left[ 1 + \frac{1}{4} \frac{f_o}{(l_a - l_g)} \left( \frac{l_a + \mu l_g}{l_a} - 1 \right) \right] \quad \dots \quad (24)$$

$$= \frac{3}{2} f_o \left[ 1 + \frac{1}{4} \frac{f_o}{l_g} \right] \quad \dots \quad (25)$$

$f/a$  has been plotted versus  $d/a$  for  $l_g/a = 0.75$  in Fig. 6, and it will be seen that there is reasonably good agreement with the measured figures. A possible explanation of this unexpected agreement is as follows:—

In calculating  $f$ ,  $V_o$  was taken to be the average potential in the grid plane, whereas the potential mid-way between the grid wires should have been used; this, in the absence of space-charge, would be greater than the average potential. On the other hand, the effect of space-charge would be to reduce the potential between the grid wires, and thus the errors arising from the two sources are seen to be in opposite senses.

## REFERENCES

- <sup>1</sup> "The Alignment of Grids in Thermionic Valves," C. S. Bull. *J. Inst. Elect. Engrs.*, Part III, June, 1945.
- <sup>2</sup> Davisson & Calbick. *Phys. Review*, August 1st, 1931.
- <sup>3</sup> Davisson & Calbick. *Phys. Review*, November 15th, 1932.
- <sup>4</sup> "Current Division in Positive Grid Triodes," Spangenberg. *Proc. Inst. Radio Engrs.*, May, 1940.
- <sup>5</sup> "Space-charge Limitations on the Focus of Electron Beams," Thompson & Headrich. *Proc. Inst. Radio Engrs.*, July, 1940.